

Gene silencing of EREG mediated by DNA methylation and histone modification in human gastric cancers

Jiyeon Yun^{1,2}, Sang-Hyun Song¹, Jinah Park^{1,3}, Hwang-Phill Kim¹, Young-Kwang Yoon¹, Kyung-Hun Lee⁴, Sae-Won Han^{1,4}, Do-Youn Oh^{1,4}, Seock-Ah Im^{1,4}, Yung-Jue Bang^{1,4} and Tae-You Kim^{1,2,4}

Epiregulin (EREG) induces cell growth by binding to the epidermal growth factor receptor (EGFR). Expression of EREG affects sensitivity to cetuximab a chimeric monoclonal antibody that inhibits the EGFR signaling pathway. The mechanism through which EREG is regulated is largely unknown, but a methyl-array study previously performed by our group revealed that EREG is methylated in gastric cancer cells. In this study, we found that EREG gene expression was low in 7 out of 11 gastric cancer cells and this downregulation was mediated by aberrant CpG methylation of the EREG promoter. Treatment with 5-aza-CdR restored EREG expression and demethylated CpG sites in the EREG promoter. Compared with DNA methyltransferase 1 (DNMT1), knock-down of DNA methyltransferase 3b (DNMT3b) significantly increased the expression of EREG and led to the demethylation of specific CpG sites in the EREG promoter, suggesting that DNMT3b primarily regulates CpG methylation and silencing of the *EREG* gene. EREG methylation was observed in 30% (4/13) of human primary gastric tumor tissues we evaluated. In addition to DNA methylation, results from a chromatin immunoprecipitation assay demonstrated that transcriptional levels of EREG were associated with the enrichment of active histone marks (H3K4me3 and ACh3) and of a repressive mark (H3K27me2). Treatment with 5-aza-CdR dynamically increased the low occupancy of H3K4me3 and ACh3, while decreasing the high enrichment of H3K27me2, indicating that dynamic histone modifications contribute to EREG regulation in addition to DNA methylation. Finally, the combination of 5-aza-CdR and cetuximab exerted a synergistic anti-proliferative effect on gastric cancer cells. Taken together, the results of our study showed for the first time that EREG is epigenetically silenced in gastric cancer cells by aberrant DNA methylation and histone modification.

Laboratory Investigation (2012) 92, 1033–1044; doi:10.1038/labinvest.2012.61; published online 16 April 2012

KEYWORDS: 5-Aza-CdR; cetuximab; DNA methylation; epiregulin (EREG); histone modification; human gastric cancer

Epiregulin (EREG) is a member of the epidermal growth factor (EGF) family, which includes heparin-binding EGF-like growth factor, transforming growth factor- α (TGF- α), epigen, amphiregulin (AREG), betacellulin and neuregulins (NRGs).¹ EREG functions as a ligand of the EGF receptor (EGFR or HER1) and HER4.^{1,2} EREG stimulates the proliferation of keratinocyte, non-transformed fibroblasts and hepatocytes; this factor is also associated with differentiation, cell migration, adhesion and facilitating new tumor blood vessels assembly in breast cancer.^{3,4} Overexpression of EREG has been observed in various cancer cells including those in the bladder, lung, kidney and colon;⁵ however, not all cancer cells have high levels of EREG expression. Other studies have reported that

EREG inhibits the growth of several tumor-derived epithelial cell lines and is not essential for the development of intestinal tumors.^{3,5} EREG has received much attention in recent years. Recently, EREG and AREG expression was found to be associated with cetuximab sensitivity. Expression of these factors may also be used to predict the outcomes of metastatic colorectal cancer patients treated with cetuximab and liver metastasis in colorectal cancer patients.^{6–9} Thus, the molecular mechanism underlying transcriptional regulation of EREG and the biological effects of EREG on tumorigenesis need to be elucidated.

Epigenetic modification, such as DNA methylation, histone modification, chromatin remodeling and micro RNA, are

¹Cancer Research Institute, Seoul National University College of Medicine, Seoul, South Korea; ²Department of Molecular Medicine and Biopharmaceutical Sciences, Graduate School of Convergence Science and Technology, Seoul National University, Seoul, South Korea; ³Korean Bioinformation Center (KOBIC), KRIBB, Daejeon, South Korea and ⁴Department of Internal Medicine, Seoul National University Hospital, Seoul, South Korea
Correspondence: Professor T-Y Kim, MD, PhD, Department of Internal Medicine, Seoul National University Hospital, 101 Daehang-ro, Jongno-gu, Seoul 110-744, South Korea.

E-mail: kimty@snu.ac.kr

Received 1 September 2011; revised 30 January 2012; accepted 13 February 2012

essential and crucial for normal cellular differentiation, development and gene expression.¹⁰ Several studies have reported abnormal epigenetic modifications associated with tumorigenesis and in various cancers.^{10,11} As these epigenetic events are reversible, abnormal alterations of these events can be used as therapeutic targets for treating cancer.¹² In particular, DNA methylation at the CpG dinucleotide has a critical role in epigenetic programming of gene expression.¹³ Many studies have shown that CpGs methylation in the promoter region is closely associated with gene silencing. Hypermethylation of tumor-suppressor genes in their promoter may strongly interfere with the binding of many transcription factors to the promoter, which regulates gene transcription and is important in the etiology of human cancers.^{14,15}

DNA methyltransferases (DNMTs) are a family of enzymes, which methylate the carbon 5 position of cytosine residues in CpG dinucleotides.¹⁶ DNMT1, -3b, -3a and -3L belong to the DNMT family.¹⁶ In general, DNMT1 is responsible for maintaining DNA methylation patterns during cell division,¹³ while DNMT3b and DNMT3a are associated with *de novo* methylation.¹⁷ In addition to DNA methylation, histone modification also helps organize nuclear architecture for the regulation of gene expression and serves as a dynamic regulator of gene activities.¹⁸ Unlike DNA methylation, covalent histone modifications are more unstable and diverse; these include post-translational modifications as acetylation, phosphorylation, methylation, sumoylation and ubiquitylation.¹⁹ To date, many studies have established that acetylation of histone lysines and methylation of lysine 4 in the histone H3 core are correlated with activation of transcriptional activity^{20,21} whereas methylation of lysine 9 and lysine 27 in the histone H3 core is closely linked to repression of transcriptional activity.²²

In this study, we found that EREG expression was silenced by aberrant promoter methylation. This was accompanied by histone modifications including low enrichment of active histone modification marks and high occupancy of repressive histone modification mark like H3K27me2. In particular, our data showed that DNA methylation of EREG was regulated by DNMT3b but not DNMT1 in gastric cancer cells. Finally, we observed that a combination of cetuximab and 5-aza-CdR reduced tumor viability *in vitro* and *in vivo*.

MATERIALS AND METHODS

Cells and Primary Human Gastric Tissues

Eleven human gastric cancer cells (SNU1, SNU5, SNU16, SNU216, SNU484, SNU601, SNU620, SNU638, SNU668, SNU719 and AGS) were obtained from the Korea Cancer Cell Bank (Seoul, South Korea). Thirteen primary human gastric tumor tissues and their matching normal tissues were obtained from Seoul National University Hospital (South Korea). After surgical removal, the tissues were immediately frozen in liquid nitrogen and stored until required.

Cell Culture and Drug Treatment

Cells were maintained in RPMI 1640 supplemented with 10% fetal bovine serum, and gentamicin (10 µg/ml) at 37 °C in a humidified 5% CO₂ atmosphere. 5-Aza-2'-deoxycytidine (5-aza-CdR; Sigma, St Louis, MO, USA) was administered every 48 h for 4 days at concentrations indicated in the figure legends and then the cells were harvested on day 5.

RT-PCR and Quantitative Real-Time RT-PCR

Total RNA was harvested with TRI Reagent (Molecular Research Center, Cincinnati, OH, USA) in accordance with the manufacturer's instructions. cDNA was synthesized from 2 µg of total RNA using ImProm-II reverse transcriptase (Promega, Madison, WI, USA) and amplified by RT-PCR using HotStart Taq (Qiagen, Hilden, Germany) with gene-specific primers. β -actin expression was used as an internal RT-PCR control. For quantitative real-time RT-PCR (qRT-PCR), cDNA was amplified using Premix Ex Taq (TaKaRa, Shiga, Japan) with SYBR Green I (Molecular Probes, Eugene, OR, USA) using a Step One Plus system (Applied Biosystems, Foster City, CA, USA). The sequences of all primers used for PCR are listed in Supplementary Table S1.

Methylation-Specific PCR, Bisulfite Sequencing and Pyrosequencing

Genomic DNA (gDNA) samples were isolated using a QIAamp DNA mini kit (Qiagen). gDNA (1 µg) was treated with sodium bisulfite and EpiTech Bisulfite (Qiagen). MSP was conducted using HotStart Taq (Qiagen) with primers specific for methylated or unmethylated sequences of the genes. Amplification conditions were as follows: 95 °C for 10 min, and 32 cycles of 95 °C for 20 s, 56 °C for 20 s and 72 °C for 20 s, followed by a final extension at 72 °C for 10 min. For bisulfite sequencing, PCR was performed as described above. The PCR products were gel purified and cloned into a TOPO TA cloning vector (Invitrogen, Carlsbad, CA, USA). The inserted PCR fragments of individual clones were sequenced. For pyrosequencing analysis, bisulfite-modified gDNA was amplified with specific primers that were biotinylated. Preparation of single-stranded DNA template, annealing to the pyrosequencing primer, and pyrosequencing were performed using PyroGold Q96 SQA reagents with a PyroMark ID pyrosequencer (Qiagen) according to the manufacturer's protocol. The pyrosequencing data were analyzed using Pyro Q-CpG software (Qiagen). All primer sequences for PCR and pyrosequencing are listed in Supplementary Table S1.

siRNA Specific for DNMT1 and DNMT3b

siRNA specific for DNMT1 and DNMT3b has been previously described²³ and control siRNA with scrambled sequences were obtained from Qiagen. Transfection of SNU601 cells was performed with Lipofectamine 2000 (Invitrogen) according to the manufacturer's instructions. Each siRNA (20 nM) were used to transfect cells every 48 h for 6 days.

Chromatin Immunoprecipitation Assay

A chromatin immunoprecipitation (ChIP) assay was performed as previously described.²⁴ Briefly, cells were cross-linked with 1% formaldehyde for 10 min at room temperature. The reaction was terminated by incubation with 0.125 M glycine for 5 min at room temperature. Nuclei were prepared and digested with 40 U MNase (Worthington Biochemical, Lakewood, NJ, USA) at 37 °C for 15 min, and were then sonicated so that the chromatin had an average fragment size of 200–400 bp. The pre-cleared chromatin was incubated overnight with antibodies at 4 °C. The chromatin was immunoprecipitated with protein A agarose (Millipore, Billerica, MA, USA), which was pre-equilibrated with sonicated salmon sperm DNA and bovine serum albumin (BSA). The immunoprecipitated materials were then washed extensively, and cross-linking was reversed. DNA from the eluted chromatin was purified by phenol extraction and ethanol precipitation. Differences in DNA enrichment of the ChIP assay samples were determined by quantitative RT-PCR using 2.5% of the precipitated sample DNA and 0.02% of the input DNA. All sequences of the EREG promoter-specific primers for the ChIP assay are listed in Supplementary Table S2.

The following antibodies were used for the ChIP assay. RNA polymerase II (Pol II; SC-899) was obtained from Santa Cruz Biotechnology (Santa Cruz, CA, USA). Anti-acetyl histone H3 (AcH3; 06-599), anti-trimethyl histone H3 (Lys4, H3K4me3; 07-473) and anti-dimethyl histone H3 (Lys27, H3K27me2; 07-452) were from Millipore.

Cell Growth Inhibition Assay

Cell growth was measured by an MTT assay as previously described.²⁵ Briefly, SNU16, SNU601 and SNU719 cells were seeded in 96-well plates and incubated at 37 °C for 24 h. The cells were then treated with 70 nM of 5-aza-CdR (Sigma) or DMSO. After 2 days, 0, 1, 10, 100 or 200 µg/ml of cetuximab alone or combination with 70 nM 5-aza-CdR was added to the cells. After 3 days, 50 µg of tetrazolium-dye (3-(4,5-dimethylthiazolyl-2)-2,5-diphenyltetrazoliumbromide, MTT; Sigma) were added to each well and the samples were then incubated for 4 h to reduce the dye. Next, the samples were treated with DMSO (Sigma) after which the absorbance of the converted dye in the living cells was measured using a microplate reader (Versa-Max, Molecular Devices, Sunnyvale, CA, USA) at a wavelength of 540 nm. Six replicate wells were used for each analysis, and at least three independent experiments were conducted.

Xenograft Mouse Model

Animal experiments were carried out in the animal facility of Seoul National University in accordance with institutional guidelines. To determine the *in vivo* activity of the combination of 5-aza-CdR and cetuximab, 4-week-old BALB/c athymic nude mice were purchased from Central Lab Animal (Seoul, South Korea). The mice were permitted to acclimatize to local conditions for 1 week before being injected with

cancer cells. Mice were injected subcutaneously with SNU601 cells in 100 µl of PBS (5×10^7 cells per 100 µl PBS). When the tumor volume reached 200 mm³, the mice were randomly divided into four groups ($n =$ eight per group) and received (day 1) vehicle, 5-aza-CdR (5.0 mg/kg) suspended in PBS, cetuximab (10 mg/kg), or a combination of the two drugs (5-aza-CdR (5.0 mg/kg) + cetuximab (10 mg/kg)) and the experimental drug administration protocol was initiated (day 1). All drugs were administered via intraperitoneal injection twice a week for 3 weeks. The tumor volume was measured every other day using calipers, and was calculated according to following formula: $((\text{width})^2 \times (\text{height}))/2$. After the final treatment (day 22), all mice were euthanized.

Western Blot Analysis

Cells were harvested and resuspended in lysis buffer with protease inhibitors. The same amount of protein (20 µg) was then obtained from each suspension and subjected to 9~13% SDS-PAGE after which the separated proteins were transferred to a nitrocellulose membrane. After blocking with buffer containing 5% skim milk plus 5% BSA, the membrane was incubated overnight with primary antibodies at 4 °C. Antibodies against p-EGFR (pY1068), p-STAT3 (pY705), p-AKT (pS473), EGFR, STAT3, AKT and caspase-3 were purchased from Cell Signaling Technology (Beverly, MA, USA). Antibodies against EREG, DNMT1 and DNMT3b were obtained from Santa Cruz Biotechnology. Anti- α -tubulin antibody was acquired from Sigma-Aldrich.

RESULTS

Loss of EREG Expression in Gastric Cancer Cells

We first examined the expression of EREG in human gastric cancer cell lines. Among the 11 gastric cancer cell lines we evaluated (Figure 1b), EREG mRNA was barely detectable in seven (SNU1, SNU16, SNU484, SNU601, SNU620, SNU719 and AGS) and highly expressed in the remaining four (SNU5, SNU216, SNU620 and SNU668). To determine whether the *EREG* gene was silenced by an epigenetic mechanism in the gastric cancer cell lines, SNU601 (which expresses low levels of EREG mRNA) and SNU668 (which expresses high levels of EREG mRNA) cells were treated with the DNA demethylating agent 5-aza-CdR. We extracted mRNA and then analyzed it by qRT-PCR (Figure 1c and Supplementary Figure S1a). This analysis showed that treatment of SNU601 cells with 5-aza-CdR increased the level of EREG mRNA by 230-fold and EREG protein expression (Figure 1c), suggesting that *EREG* may be silenced by DNA methylation in SNU601 cells. We also found that EREG mRNA expression in SNU601 cells gradually increased in a time-dependent manner following 5-aza-CdR treatment (Figure 1d and Supplementary Figure S1b).

We then confirmed the recovery of EREG mRNA expression in gastric cancer cell lines with endogenously low or high levels of EREG mRNA after 5-aza-CdR treatment. RT-PCR analysis showed that *EREG* gene expression was significantly increased in SNU601, SNU620, SNU719 and AGS cells by

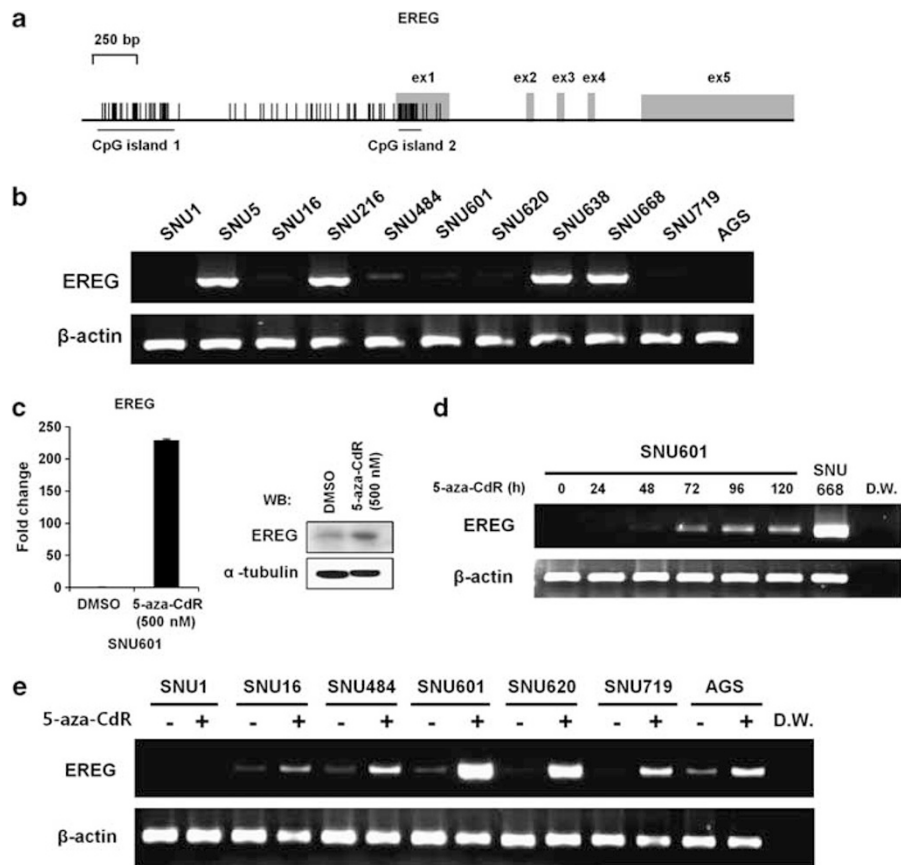


Figure 1 Loss of EREG expression in human gastric cancer cells. (a) Schematic representation of the *EREG* gene. Exons of the *EREG* gene are indicated by shaded boxes. Vertical bars represent each CpG site. Two putative CpG islands are indicated. (b) EREG mRNA from 11 gastric carcinoma cells was analyzed by RT-PCR. β -actin mRNA served as an internal control. (c–e) Restoration of EREG expression after 5-aza-CdR treatment. (c) The levels of EREG mRNA and protein in SNU601 cells were measured by qRT-PCR and western blotting, respectively, after treatment with 500 nM of 5-aza-CdR or DMSO for 5 days. In the graph showing EREG mRNA levels, each value was normalized relative to that of β -actin. Error bars represent the s.d. for several independent RNA preparations. (d) SNU601 cells were treated with 500 nM of 5-aza-CdR and analyzed over a 5-day time course; EREG mRNA was analyzed every day by RT-PCR. (e) Cells were treated for 5 days with DMSO or 500 nM of 5-aza-CdR as indicated. Total RNA was isolated to measure the recovery of EREG expression.

5-aza-CdR treatment. *EREG* gene expression was slightly increased by 5-aza-CdR treatment in SNU1, SNU16 and SNU484 cells (Figure 1e). In contrast, no change in the expression of EREG mRNA was observed following 5-aza-CdR treatment (Supplementary Figure S1c) in cells (SNU668) with endogenously high levels of EREG mRNA. These results suggest that DNA methylation may have an important role in *EREG* gene silencing in human gastric cancer cells.

Correlation of EREG Promoter Methylation with Transcriptional Silencing

To determine whether the silencing of EREG expression was due to promoter methylation, we examined the methylation status of the EREG promoter region in SNU601 and SNU668 cells using MSP (Figure 2a), which covered the regions within -1650 to -1350 (region 1), -380 to -224 (region 2) and $+101$ to $+263$ (region 3). Results of the MSP assay revealed distinct differences in CpG methylation of the EREG promoter between SNU601 and SNU668 cells. In region 2 and 3

of the EREG promoter, a methylated band (lanes indicated by M) was identified in SNU601 cells whereas an unmethylated band (lanes indicated by U) was observed in SNU668 cells. As there was no significant difference in CpG methylation between the two cell lines in region 1, we excluded region 1 of EREG promoter from the analysis.

To confirm the MSP assay results and determine the precise methylation status of the EREG promoter, we performed bisulfite sequencing of regions 2 and 3. We also evaluated region 4 that was located between regions 2 and 3 of the EREG promoter (Figure 2b). Consistent with the MSP data, regions 2 and 3 of the promoter were highly methylated in SNU601 cells while these regions were unmethylated in SNU668 cells. To further quantify EREG promoter methylation, we measured the percentage of CpG methylation in the promoter in SNU601 and SNU668 cells by pyrosequencing analysis (Figure 2c). Two different primers corresponding to sequences located in regions 2 or 4 were used for this procedure. Consistent with the bisulfite sequencing data,

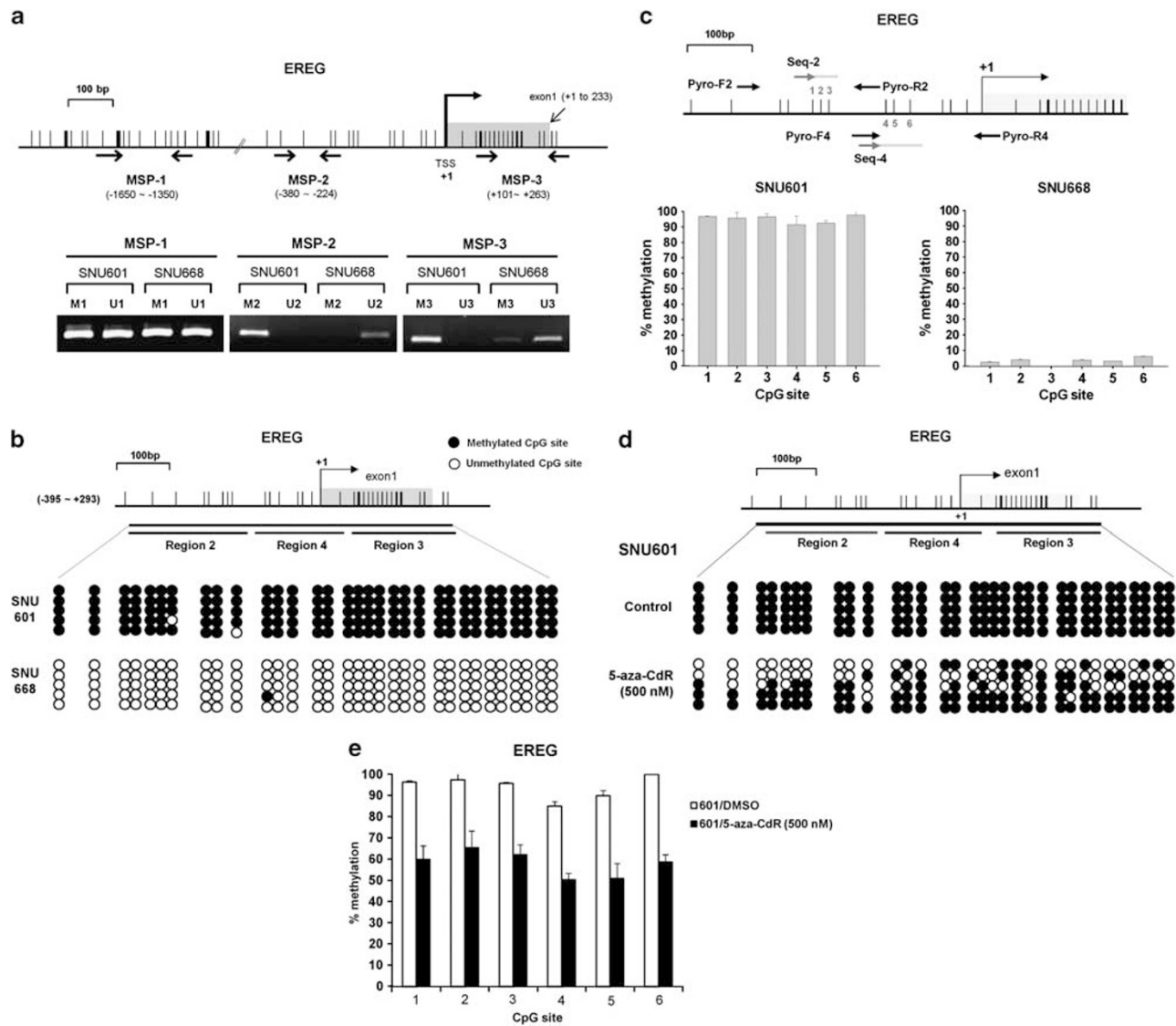


Figure 2 Positive correlation of DNA methylation with transcriptional silencing of EREG. **(a)** Methylation-specific PCR (MSP) of EREG. The approximate locations and directions of the MSP primers for each region are indicated by arrows. Bisulfite-modified gDNA derived from EREG-negative SNU601 cells and EREG-positive SNU668 cells were amplified with primers specific for unmethylated (U) or methylated (M) DNA. **(b)** Bisulfite genomic sequencing analysis of the EREG promoter in the SNU601 and SNU668 cells. Each row of circles represents a single plasmid cloned and sequenced from PCR products generated by the amplification of bisulfite-treated DNA. Open and closed circles represent unmethylated and methylated CpG sites, respectively. **(c)** Quantitative analysis of EREG DNA methylation. The methylation ratio of EREG in SNU601 and SNU668 cells was determined by pyrosequencing. Locations of sequences corresponding to the two primer sets used for pyrosequencing are indicated by arrows. The x and y axis represent each CpG position in the EREG promoter and percentage of CpG methylation, respectively. Error bars represent the s.d. for several independent preparations of bisulfite-treated gDNA. **(d, e)** Demethylation of the EREG promoter by 5-aza-CdR. SNU601 cells were treated with DMSO or 500 nM of 5-aza-CdR for 5 days and gDNA was then isolated for **(d)** bisulfite genomic sequencing or **(e)** pyrosequencing analysis. Data are presented as the mean \pm s.d.

SNU601 cells showed about 95% CpG methylation in the pyrosequencing analysis. However, only 2% of CpGs were methylated in SNU668 cells.

To investigate whether the methylation of EREG was limited only in SNU601 and SNU668, we next quantified EREG methylation in other gastric cancer cell lines. Cells with low levels of EREG expression (SNU1, SNU601, SNU620, SNU719 and AGS) were shown to have a high percentage of CpG methylation in the promoter (Supplementary Figure

S2a). Interestingly, SNU16 and SNU484 cells (ones with low expression of EREG mRNA) had an intermediate percentage of CpG methylation (about 45%) in region 2 but a low percentage (below 20%) in region 4. Cells with naturally high levels of EREG expression (SNU5, SNU216, SNU638 and SNU668) had a low percentage of CpG methylation (Supplementary Figure S2b). Most gastric cancer cells showed a close inverse correlation between the expression level of EREG and CpG methylation in the promoter. Therefore, our

results suggest that the CpG sites in the EREG promoter, especially in region 2, may have an important role in CpG methylation-related gene silencing of EREG.

To further investigate CpG methylation-mediated transcriptional silencing of EREG, SNU601 cells were treated with 5-aza-CdR. Using a bisulfite sequencing assay, we showed that 500 nM of 5-aza-CdR caused a statistically significant reduction ($*P < 0.05$) in EREG promoter methylation, from 95 to 50% overall (Figure 2d). Consistent with the bisulfite sequencing results, pyrosequencing analysis also showed that treatment with 500 nM of 5-aza-CdR led to decreased EREG promoter demethylation of about 50% (Figure 2e), suggesting that the restoration of EREG mRNA expression following 5-aza-CdR treatment was caused by significant demethylation of the hypermethylated CpG sites in the EREG promoter.

Recovery of Expression and Demethylation of the EREG Gene by Transient DNMT3b Silencing

DNA methylation is initiated by methyltransferases, DNMT3a and DNMT3b, which use unmethylated DNAs as the substrate for *de novo* methylation.^{26,27} DNMT3b is directly associated with many human diseases including cancer.^{28,29} For example, upregulation of DNMT3b expression is observed in sporadic breast carcinoma and acute myeloid leukemia while DNMT1 and DNMT3a levels are reduced.³⁰ DNMT3b is also overexpressed and linked to the CpG island methylator phenotype in colon cancer.³¹ Each DNMT (DNMT1, DNMT3a and DNMT3b) is recruited with some proteins, such as methyl CpG-binding protein and histone deacetylase, to distinct chromosomal regions.³² DNMT3b is known to regulate and target specific genes.^{29,33}

To determine which DNMTs are associated with EREG promoter methylation, SNU601 cells were transiently transfected with 20 nM of control, DNMT1- or DNMT3b-specific siRNA. The level of gene expression and methylation status of the *EREG* gene were determined. The levels of DNMT1 and DNMT3b decreased $> 50\%$ in DNMT1 or DNMT3b knock-down SNU601 cells, respectively (Figures 3a and b, and Supplementary Figure S3a). As we previously reported that the levels of RASSF1A mRNA were restored and demethylated in transient DNMT1 knock-down SNU601 cells,²³ we examined the induction and demethylation of RASSF1A to confirm that DNMT1 or DNMT3b were efficiently and specifically knocked-down in the SNU601 cells (Figure 3d). Figure 3d shows the restoration of RASSF1A mRNA expression in DNMT1 knock-down SNU601 cells. However, we did not observe the induction of RASSF1A expression in DNMT3b knock-down SNU601 cells. We also observed demethylation of the RASSF1A promoter in DNMT1 knock-down SNU601 but not in DNMT3b-deficient cells (Supplementary Figure S3b). These results suggested that DNMT1 and DNMT3b expression was efficiently reduced in SNU601 cells. Under these conditions, we found that EREG mRNA expression was restored in DNMT3b-deficient SNU601, not in DNMT1-deficient cells (Figures 3c and d). To determine

the DNA methylation status of the EREG promoter in the DNMT1- and DNMT3b-deficient cells, bisulfite sequencing of the EREG promoter was performed. In DNMT3b-deficient SNU601 cells, we observed the demethylation of specific CpG sites in the EREG promoter. However, we did not identify as many demethylated CpG site as in DNMT1-deficient SNU601 cells as in DNMT3b-deficient cells (Figure 3e). We also confirmed these findings in other gastric cancer cell lines (AGS and SNU719) expressing low levels of EREG (Supplementary Figures S3c and d). Taken together, these results strongly suggested that DNMT3b is closely associated with extensive methylation of the EREG promoter that results in the silencing of EREG expression.

Methylation Status and EREG mRNA Levels in Primary Gastric Tumor Tissues

We determined whether DNA methylation-mediated transcriptional silencing of EREG also occurs in primary gastric tumor tissues. First, pyrosequencing analysis revealed that region 2 of the EREG promoter was hypermethylated (40~80%) in 4 out of 13 (30%) primary gastric tumor tissues. However, low levels of CpG methylation ($< 40\%$) were found in region 4 (Figure 4a). Compared with the extensive methylation observed in the tumor tissues, the matched normal gastric tissues showed $< 20\%$ CpG methylation in the EREG promoter, suggesting that EREG promoter methylation is not a cell line-specific event (Figure 4a and Table 1). Consistent with CpG methylation status, low levels of EREG expression were detected by qRT-PCR and western blotting in primary gastric tumor tissues in which the EREG promoter was methylated (Figures 4b and c, respectively), suggesting that about 30% of gastric cancer patients lacked EREG expression because of cancer-specific aberrant DNA methylation of the EREG promoter. We also found that EREG mRNA expression was lower than average in 13 primary gastric tumor tissues compared with their matching normal tissues (Figure 4d).

Accumulation of Active Histone Modifications after 5-Aza-CdR Treatment

As histone modifications and DNA methylation cooperatively interact to regulate gene expression at multiple levels,³¹ we investigated whether DNA methylation status of the EREG promoter also affects histone modifications around the *EREG* gene. First, we evaluated the recruitment of RNA polymerase II (Pol II) and histone modification status around the *EREG* gene by a ChIP assay and qRT-PCR in SNU601 and SNU668 cells. The association of Pol II within the *EREG* gene coincided with robust enrichment of acetylated histone H3 (AcH3) and H3K4 tri-methylation (H3K4me3), consistent with active transcription of *EREG* in SNU668 cells (Figure 5a). Similar to the absence of EREG expression, ChIP analysis revealed that Pol II, AcH3 and H3K4me3 levels were barely detectable at the EREG promoter region in SNU601 cells (Figure 5a). H3K27 di-methylation (H3K27me2), a repressive histone modification mark, was

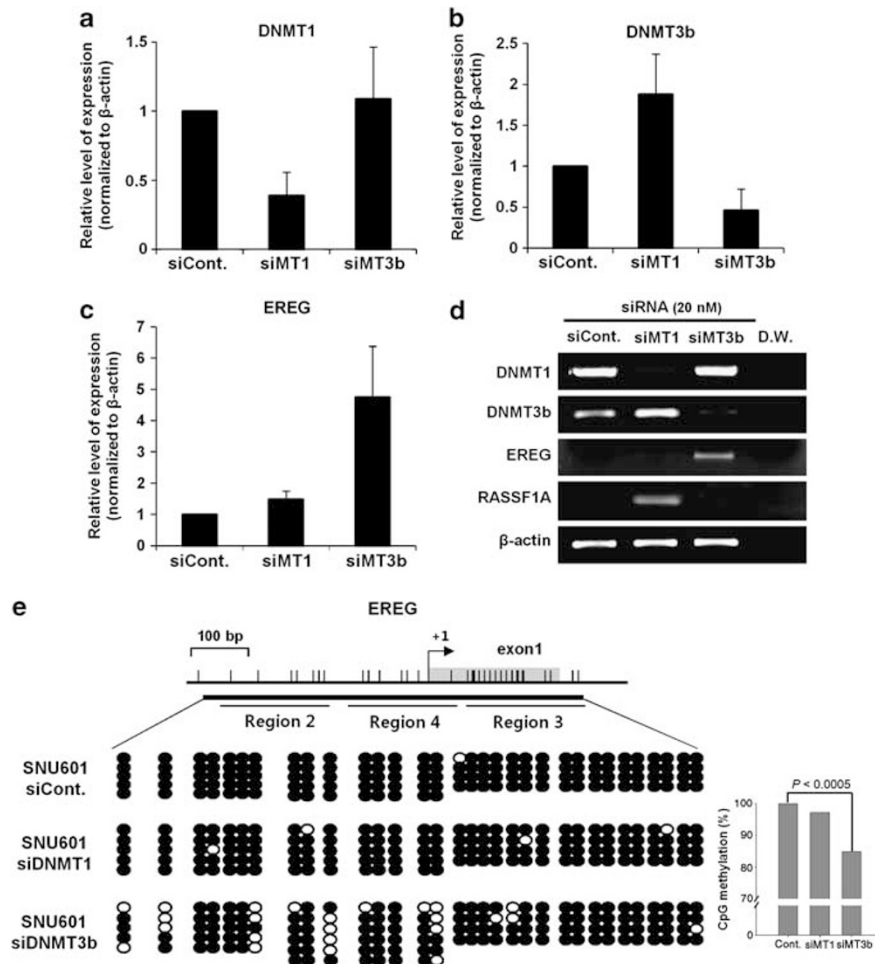


Figure 3 Restoration of EREG expression by DNMT3b depletion. SNU601 cells were transfected with control siRNA, or siRNA specific for DNMT1 or DNMT3b (20 nM) and harvested after 6 days. qRT-PCR was performed to measure (a) DNMT1, (b) DNMT3b and (c) EREG expression. Data are expressed as the mean \pm s.d. (d) RASSF1A expression was analyzed by RT-PCR. (e) siRNA-transfected cells were used for bisulfite genomic sequencing analysis as described in the legend for Figure 2. These experiments were conducted at least in triplicate and the results of a representative experiment are shown. The statistical significance of EREG demethylation by DNMT3b knock-down was calculated using an unpaired Student's *t*-test and the *P*-value was <0.0005 .

significantly lower in SNU668 cells compared with SNU601 cells, similar to EREG expression.

To further elucidate the DNA methylation-mediated histone tail modification patterns, SNU601 cells containing the methylated *EREG* gene were treated with 500 nM of 5-aza-CdR to restore EREG expression. On exposure to 5-aza-CdR, the levels of both Pol II and H3K4me3 in the EREG promoter region markedly increased and the level of H3K27me2 slightly decreased, indicating that methylated DNA is correlated with transcriptional repression (Figure 5b). Taken together, these results suggested that hypermethylation of the EREG promoter associated with histone modifications induced the inactivation of *EREG* gene expression.

Cytotoxicity of Cetuximab Enhanced by 5-Aza-CdR Induction of EREG Expression

Cetuximab, a monoclonal antibody that inhibits EGFR, binds to the extracellular domain of the receptor and prevents

ligand binding; this subsequently abolishes activation of the receptor tyrosine kinase activity.³⁴ Although cetuximab is considered to be a promising molecular targeting agent, this inhibitor does not significantly reduce cell proliferation in solid tumors. Therefore, many groups have investigated the combination of cetuximab with other drugs to enhance therapeutic efficacy.^{35,36} Interestingly, the effect of cetuximab can be enhanced in cells with high levels of EGFR ligands such as EREG and AREG.^{3,5} However, the results from this study showed that many gastric cancer cells did not express EREG because of aberrant DNA methylation. We therefore determined whether the restoration of EREG expression by 5-aza-CdR treatment in EREG-negative cells might enhance the cytotoxicity of cetuximab.

First, we tested a range of concentrations of 5-aza-CdR that could be used in combination with different concentrations of cetuximab to identify the non-cytotoxic levels of 5-aza-CdR. We determined that the appropriate dose of 5-aza-CdR not

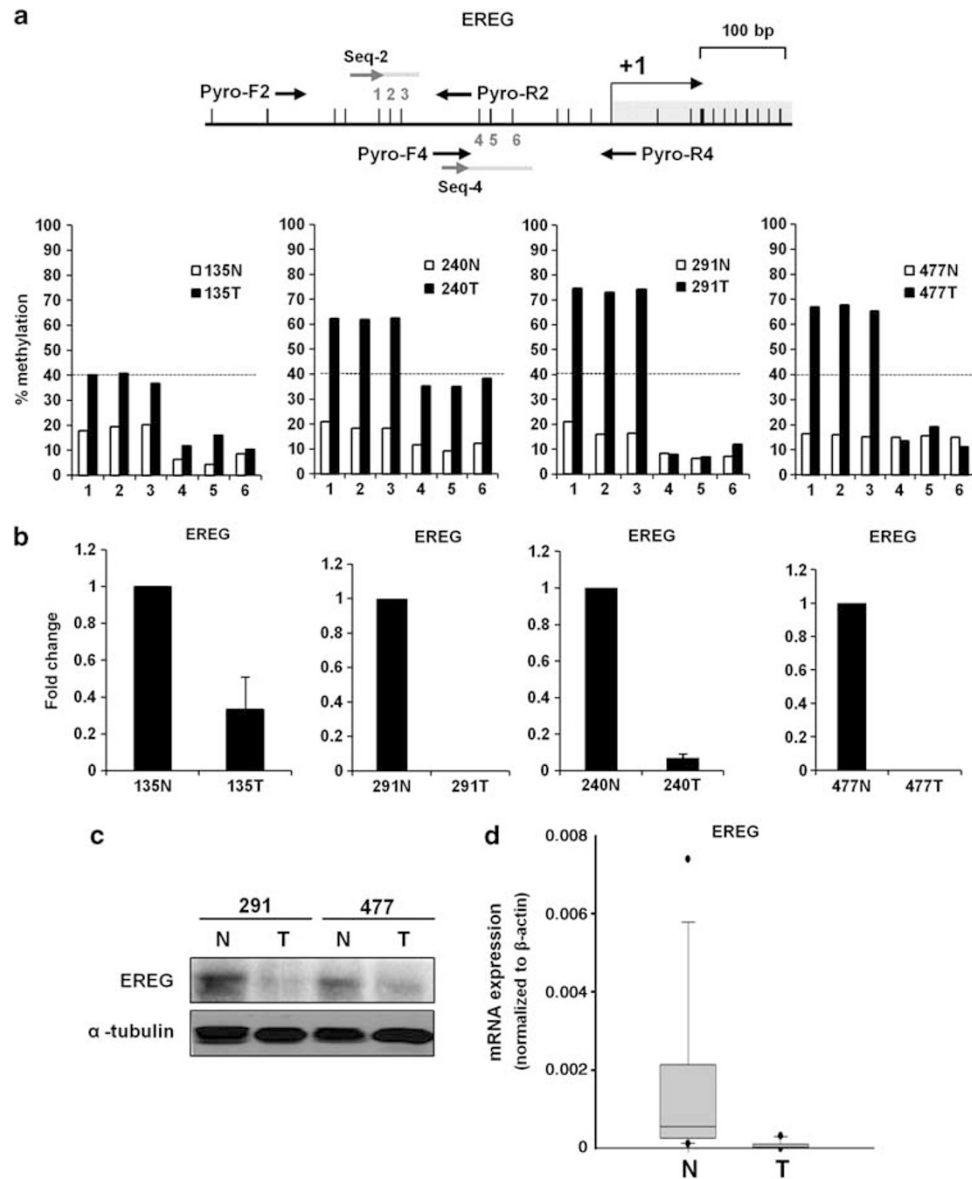


Figure 4 Methylation status of the EREG promoter in human primary gastric tissues. gDNA and mRNA were extracted from 13 normal human primary gastric tissues and their matched tumor tissues (**a**). Bisulfite-treated gDNA was used to determine the methylation ratio of the EREG promoter by pyrosequencing. The dotted line represents the cutoff for the percentage of acceptable CpG methylation (40%) in the EREG promoter. (**b**) The level of EREG expression in the samples analyzed in panel **a** was determined by qRT-PCR and expressed as a fold change relative to normal tissue samples. EREG expression was normalized to β -actin mRNA. Data are expressed as the mean \pm s.d. (**c**) The protein level of EREG in the primary samples analyzed in panel **a** was measured using western blot assay. (**d**) Loss of EREG expression in gastric tumor tissues. A summary of EREG expression in 13 normal and cancerous primary gastric tissues is shown and presented as box plots of relative expression; the median (s.d.) is also shown ($*P < 0.05$). N, normal tissues; T, tumor tissues.

associated with any cytotoxicity was 70 nM (Supplementary Figures S4b–d). To further verify whether 70 nM of 5-aza-CdR sufficiently induced EREG mRNA and protein expression, we confirmed our findings using qPCR and western blotting (Supplementary Figure S4a). Cells with low levels of EREG expression (SNU601, SNU16 and SNU719) were incubated with 70 nM 5-aza-CdR (or DMSO as a control). After 2 days, 1–200 μ g/ml cetuximab alone or 1–200 μ g/ml cetuximab combined with 70 nM of 5-aza-CdR was added to the cells for 3 days. Interestingly, we observed that cell viability notably

decreased among cells treated with a combination of cetuximab and 5-aza-CdR (Figures 6a–c). Furthermore, exposure to the combination of cetuximab and 5-aza-CdR after pre-treatment with 5-aza-CdR resulted in a significant reduction of cells growth. To further verify changes in EGFR signaling, we conducted an immunoblot analysis (Supplementary Figure S4e). Although phospho-EGFR was increased with a combination of cetuximab and 5-aza-CdR after pre-treatment of 5-aza-CdR, phospho-AKT, a key downstream signaling effector of EGFR, was significantly inhibited.

Table 1 Methylation of EREG in normal and cancerous primary gastric tissue samples

| Normal tissue samples | | | Cancer tissue samples | | |
|-----------------------|------------|-------------|-----------------------|------------|--------------|
| % Methylation | Region 2 | Region 4 | % Methylation | Region 2 | Region 4 |
| 0 < % < 20 | 7/13 (54%) | 11/13 (85%) | 0 < % < 20 | 7/13 (54%) | 13/13 (100%) |
| 20 < % < 40 | 2/13 (15%) | 2/13 (15%) | 20 < % < 40 | 6/13 (46%) | 0/13 (0%) |
| 40 < % < 60 | 1/13 (8%) | 0/13 (0%) | 40 < % < 60 | 0/13 (0%) | 0/13 (0%) |
| 60 < % < 80 | 3/13 (23%) | 0/13 (0%) | 60 < % < 80 | 0/13 (0%) | 0/13 (0%) |
| 80 < % < 100 | 0/13 (0%) | 0/13 (0%) | 80 < % < 100 | 0/13 (0%) | 0/13 (0%) |

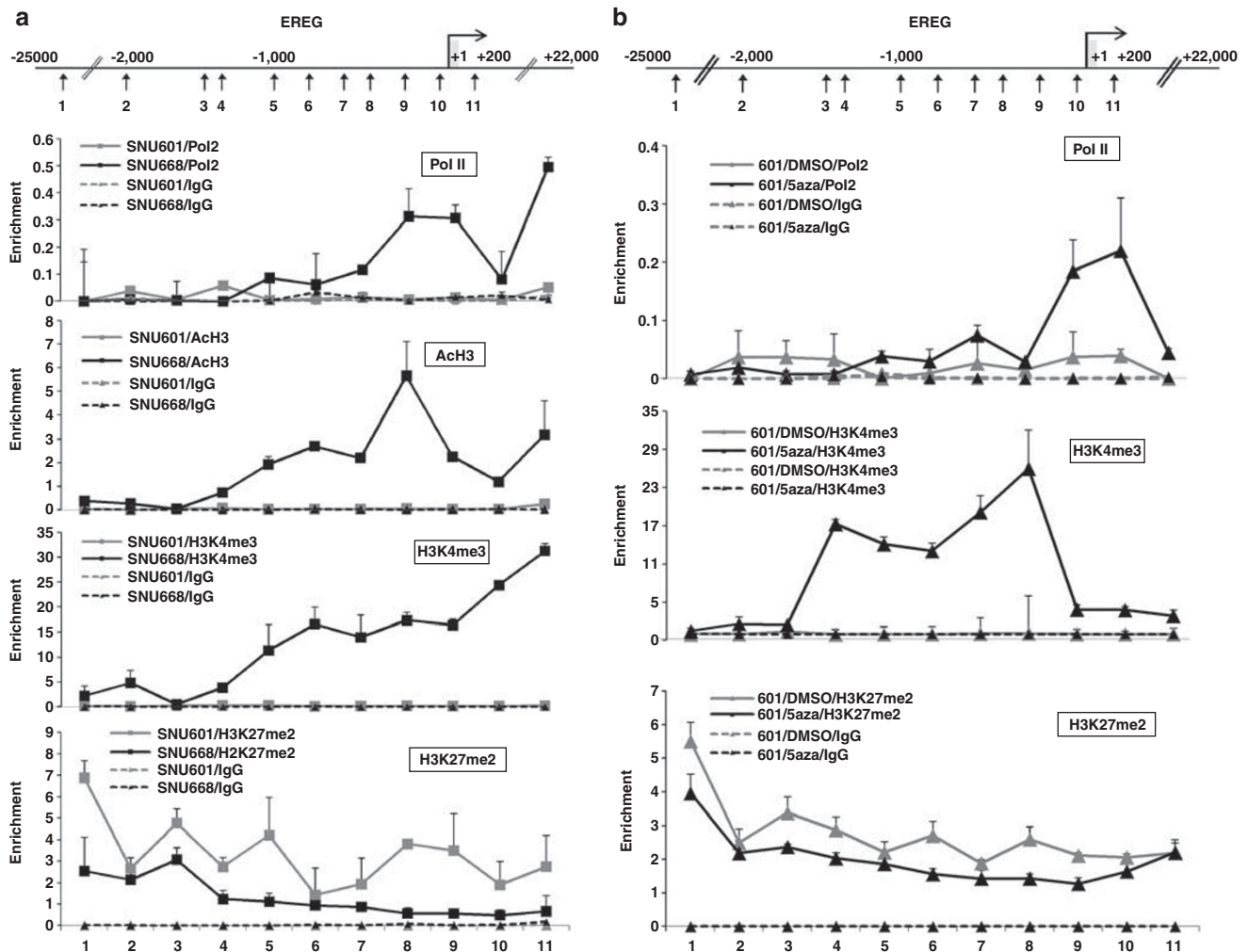


Figure 5 Enrichment of active histone modifications in the *EREG* gene following 5-aza-CdR treatment. (a) Characterization of chromatin modification patterns around the *EREG* gene. A ChIP assay was performed in SNU601 and SNU668 cells using antibodies specific for Pol II, AcH3, H3K4me3, H3K27me2 or control IgG. Enrichment was measured by qRT-PCR and reported relative to the total input (4%). The results for at least three chromatin preparations are shown \pm s.e.m. (b) Restoration of active histone modification markers after 5-aza-CdR treatment. Chromatin was prepared from SNU601 cells and treated with DMSO or 5-aza-CdR (500 nM) for 5 days. A ChIP assay was performed with antibodies targeting Pol II, H3K4me3 and H3K27me2. Data are presented as the mean \pm s.e.m.

Subsequently, we observed the effects of a combination of cetuximab and 5-aza-CdR on apoptosis. The level of cleaved caspase-3 was increased with the combination treatment (Supplementary Figure S4e). Interestingly, we found that a

combination of cetuximab and 5-aza-CdR along with 5-aza-CdR pre-treatment greatly induced the cleavage of caspase-3, suggesting that treatment with cetuximab and 5-aza-CdR strongly induced cell apoptosis. In addition, increased

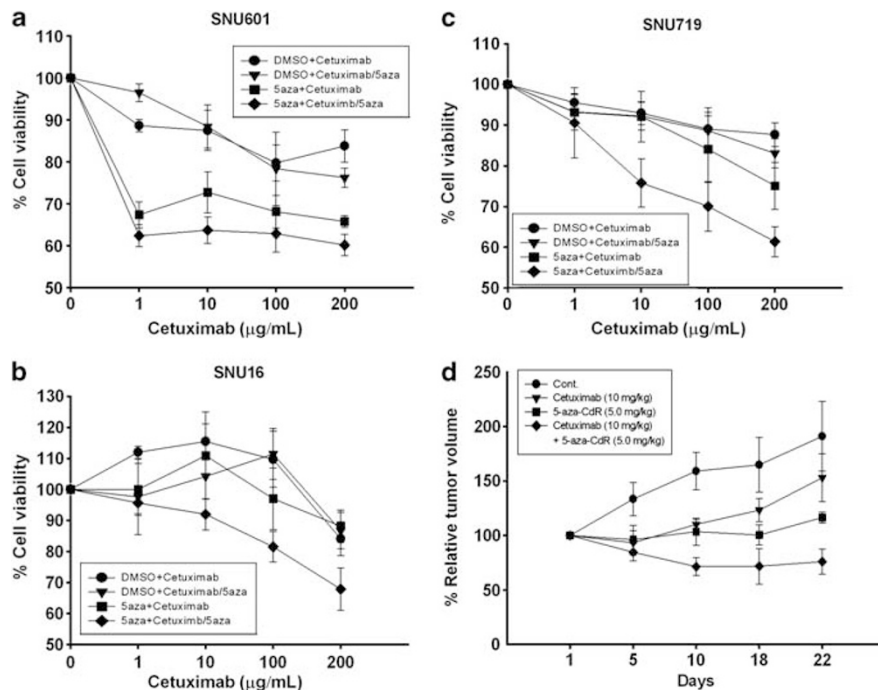


Figure 6 Enhanced cytotoxicity of cetuximab by 5-aza-CdR. Treatment with 5-aza-CdR enhanced the anti-proliferative activity of cetuximab. Cells were pre-treated with DMSO or 5-aza-CdR (70 nM) for 2 days and then exposed to increasing concentrations (1, 10, 100 and 200 µg/ml) of cetuximab alone or combined with 5-aza-CdR (70 nM). After 3 days, the viability of (a) SNU601, (b) SNU16 and (c) SNU719 cells was determined with an MTT assay. The x axis represents the dose of cetuximab (µg/ml) and y axis denotes the relative cell viability expressed as a percentage relative to the DMSO-treated control cells. ●, DMSO (pre-treatment) + cetuximab only; ▼, DMSO + cetuximab/5-aza-CdR (combination); ■, 5-aza-CdR + cetuximab only; ◆, 5-aza-CdR + cetuximab/5-aza-CdR. (d) SNU601 cells were injected s.c. into nude mice randomly divided to four groups ($n = 8$). Treatment with 5-aza-CdR (5.0 mg/kg delivered via intraperitoneal (i.p.) twice weekly for 3 weeks) and cetuximab (10 mg/kg via i.p. twice weekly for 4 weeks) was initiated once the tumor volume reached 100 mm³. Tumor volume was measured three times weekly until the group tumor volume reached the predetermined endpoint of 500 mm³. The x axis represents the days after initiated drug treatment and y axis represents the relative tumor volume (%). Bars represent the s.e. Repeated measures analyzed by an ANOVA indicated statistically significant effects ($P < 0.05$) in all groups. ●, control; ▼, cetuximab (10 mg/kg); ■, 5-aza-CdR (5.0 mg/kg); and ◆, 5-aza-CdR (5.0 mg/kg) + cetuximab (10 mg/kg).

numbers of apoptotic cells were detected by Annexin V assay (Supplementary Figure S4f).

Finally, we tested the effects of treatment with a combination of 5-aza-CdR and cetuximab using SNU601 xenograft model (Figure 6d). We found that treatment with cetuximab and 5-aza-CdR (combination group) completely inhibited tumor growth in the SNU601-bearing mice. However, significant growth inhibition was not detected in mice treated with cetuximab alone or 5-aza-CdR alone. Taken together, our results give a rise a new concept that combinational treatment with 5-aza-CdR and cetuximab may be an effective therapeutic strategy for treating cancer.

DISCUSSION

Compared with other EGF family members such as EGF, TGF or NRGs, the biological function of EREG (an EREG ligand) has not been extensively studied. In many human cancers, EREG is overexpressed, and promotes cell growth and migration.^{37,38} EREG also increases cell differentiation and survival. However, some studies have shown that EREG inhibits the growth of tumor-derived epithelial cell lines.² Recently, it was shown that the cytotoxic effects of cetuximab

are strongly correlated with the expression levels of EREG and AREG, another ligand of EGFR.^{6,7} Thus, EREG is considered to be a putative biomarker that may help predict outcomes and disease control in colorectal cancer patients treated with cetuximab.^{6,7} However, no studies have been conducted to elucidate the role of EREG in gastric cancer development.

In this study, we investigated the regulatory mechanisms of EREG expression in human gastric cancer to identify a new biomarker for establishing an effective cancer treatment strategy based on epigenetic status. We found that expression of EREG was significantly silenced in human gastric cancer cells (60%) and primary gastric tumor tissues (30%) because of aberrant DNA methylation of the EREG promoter. Although the EREG promoter was not methylated in gastric cancer cells with a high level of EREG expression (SNU5, SNU216, SNU638 and SNU668), hypermethylation around the EREG promoter region (Figure 2) was observed in cells lacking EREG expression (SNU1, SNU601, SNU620, SNU719 and AGS). In cells with intermediate levels of EREG expression (SNU16 and SNU484), about 40% CpG methylation in region 2 of the EREG promoter region was observed

(Supplementary Figure S2). Region 2 is located 200-bp upstream of the *EREG* gene transcription start site. In contrast, <10% of the CpG sites in region 4, which is sequentially located downstream of region 2, were methylated in SNU16 and SNU484 cells lacking *EREG* expression, indicating that the level of *EREG* transcription is strongly associated with methylation in region 2 of the *EREG* promoter (Figure 2 and Supplementary Figure S2).

DNA methylation is catalyzed by DNMTs.¹⁶ To identify which DNMT specifically contributes to *de novo* *EREG* promoter methylation, the dependency of *EREG* methylation on each DNMT was evaluated by transient DNMT knock-down with siRNA using a previously described technique.¹⁶ Loss of DNMT3b, but not DNMT1, led to demethylation and recovered expression of silenced *EREG* in SNU601 cells, supporting the hypothesis that methylation of the *EREG* promoter is mainly regulated by DNMT3b. As restoration of demethylation following DNMT3b depletion (Figure 3) was less significant than that observed after treatment with 5-aza-CdR (a DNA demethylating agent), we cannot exclude the possibility that other DNMTs may have partially contributed to *EREG* promoter methylation. We also confirmed the knock-down of DNMT1 and DNMT3b; however, the siRNA-induced knock-down of DNMT3b induced a twofold increase in DNMT1 mRNA (Figure 3). This result is consistent with that of a previous report²³ and may be caused by compensation for DNMT3b reduction. As increased DNMT1 levels can interfere with the effect of DNMT3b depletion, further study is therefore required to assess compensatory mechanisms involving both DNMTs.

It has been shown that histone modifications are often associated with DNA methylation.^{39,40} Concurrent with this finding, our results showed that transcriptional silencing of *EREG* was strongly correlated with repressive histone modification marks such as deacetylation of histones H3, loss of H3K4me3 and gain of H3K27me2 (Figure 4). Moreover, we found that treatment of SNU601 cells with 5-aza-CdR led to a remarkable increase in H3K4me3 occupancy and a minor decrease in H3K27me2 around the *EREG* gene. These findings suggested that DNA methylation in the *EREG* promoter region can directly affect histone modification patterns and significantly repress *EREG* expression. Thus, functional activation of H3K4 methyltransferases MLL1, 2 and 3, and Set7/9 [ref. 41] as well as concomitant treatment with a demethylating agent may synergistically induce the transcription of aberrantly silenced *EREG* genes.

Data from our present study on the regulatory mechanisms of *EREG* also have potential implications for the combined use of a demethylating agent with cetuximab, a well-known EGFR inhibitor, in clinical settings.⁴² Recently, it has been reported that colorectal cancer cells with high levels of *EREG* and *AREG* are more sensitive to cetuximab than cells with low expression.^{6,7} Based on these studies, we hypothesized that the combination of 5-aza-CdR and cetuximab exerts a synergistic antitumor effect on cells lacking

EREG expression via DNA methylation. As expected, combined treatment with cetuximab and 5-aza-CdR enhanced cytotoxicity and led to apoptosis *in vitro* and in the *in vivo* model (Figure 6 and Supplementary Figure S4e). Moreover, we found that relative to treatment with cetuximab alone, pre-treatment with 5-aza-CdR significantly enhanced the cytotoxicity of cetuximab and decreased the viability of gastric cancer cells in which *EREG* is methylated. Therefore, restoration of *EREG* expression by a demethylating agent in cancer cells lacking *EREG* expression may enhance sensitivity to cetuximab although 5-aza-CdR is associated with non-specific effects in these cells. Thus, our observations add new insight into the mechanisms underlying cancer therapies that increase the efficiency of targeted anticancer drugs, including cetuximab, with low-dose 5-aza-CdR treatment.⁴³

In summary, we identified the molecular mechanism of *EREG* transcriptional silencing in human gastric cancer. *EREG* expression was markedly downregulated by aberrant DNA methylation and accompanied by repressive histone modification marks. Loss of *EREG* expression was found in 60% (7/11) of human gastric cancer cells and 30% (4/13) of primary gastric tumor tissues examined in our study. *EREG* expression was inversely correlated with CpG methylation of the *EREG* promoter. Restoration of *EREG* expression by 5-aza-CdR impaired promoter methylation, which was mostly targeted by DNMT3b but not DNMT1, and increased the appearance of active histone modification marks associated with *EREG* expression. Furthermore, treatment with 5-aza-CdR followed by cetuximab resulted in a significant antitumor effect on cetuximab-resistant gastric cancer cells. Taken together, our results indicated that the epigenetic properties of the *EREG* gene may be harnessed in combination with the use of other appropriate drugs for establishing effective anticancer treatments.

Supplementary Information accompanies the paper on the Laboratory Investigation website (<http://www.laboratoryinvestigation.org>)

ACKNOWLEDGEMENT

This research was supported by a Grant (no. 0720540) from the National R&D Program for Cancer Control, Ministry of Health, Welfare and Family Affairs, South Korea, and by a Grant (no. R31-2008-000-10103-0) from the WCU project of the MEST and NRF.

DISCLOSURE/CONFLICT OF INTEREST

The authors declare no conflict of interest.

1. Komurasaki T, Toyoda H, Uchida D, *et al*. Epiregulin binds to epidermal growth factor receptor and ErbB-4 and induces tyrosine phosphorylation of epidermal growth factor receptor, ErbB-2, ErbB-3 and ErbB-4. *Oncogene* 1997;15:2841–2848.
2. Eltarhouny SA, Elsayy WH, Radpour R, *et al*. Genes controlling spread of breast cancer to lung "gang of 4". *Exp Oncol* 2008;30:91–95.
3. Inatomi O, Andoh A, Yagi Y, *et al*. Regulation of amphiregulin and epiregulin expression in human colonic subepithelial myofibroblasts. *Int J Mol Med* 2006;18:497–503.
4. Gupta GP, Nguyen DX, Chiang AC, *et al*. Mediators of vascular remodelling co-opted for sequential steps in lung metastasis. *Nature* 2007;446:765–770.

5. Lee D, Pearsall RS, Das S, *et al*. Epiregulin is not essential for development of intestinal tumors but is required for protection from intestinal damage. *Mol Cell Biol* 2004;24:8907–8916.
6. Jacobs B, De Rooock W, Piessevaux H, *et al*. Amphiregulin and epiregulin mRNA expression in primary tumors predicts outcome in metastatic colorectal cancer treated with cetuximab. *J Clin Oncol* 2009;27:5068–5074.
7. Khambata-Ford S, Garrett CR, Meropol NJ, *et al*. Expression of epiregulin and amphiregulin and K-ras mutation status predict disease control in metastatic colorectal cancer patients treated with cetuximab. *J Clin Oncol* 2007;25:3230–3237.
8. Saridakis Z, Tzardi M, Papadakis C, *et al*. Impact of KRAS, BRAF, PIK3CA mutations, PTEN, AREG, EREG expression and skin rash in $>/= 2$ line cetuximab-based therapy of colorectal cancer patients. *PLoS One* 2011;6:e15980.
9. Watanabe T, Kobunai T, Yamamoto Y, *et al*. Prediction of liver metastasis after colorectal cancer using reverse transcription-polymerase chain reaction analysis of 10 genes. *Eur J Cancer* 2010;46:2119–2126.
10. Wozniak RJ, Klimecki WT, Lau SS, *et al*. 5-Aza-2'-deoxycytidine-mediated reductions in G9A histone methyltransferase and histone H3 K9 di-methylation levels are linked to tumor suppressor gene reactivation. *Oncogene* 2007;26:77–90.
11. Park J, Song SH, Kim TY, *et al*. Aberrant methylation of integrin alpha4 gene in human gastric cancer cells. *Oncogene* 2004;23:3474–3480.
12. Kelly TK, De Carvalho DD, Jones PA. Epigenetic modifications as therapeutic targets. *Nat Biotechnol* 2010;28:1069–1078.
13. Pai AA, Bell JT, Marioni JC, *et al*. A genome-wide study of DNA methylation patterns and gene expression levels in multiple human and chimpanzee tissues. *PLoS Genet* 2011;7:e1001316.
14. Hatziaepostolou M, Iliopoulos D. Epigenetic aberrations during oncogenesis. *Cell Mol Life Sci* 2011;68:1681–1702.
15. Jones PA, Baylin SB. The epigenomics of cancer. *Cell* 2007;128:683–692.
16. Kim H, Park J, Jung Y, *et al*. DNA methyltransferase 3-like affects promoter methylation of thymine DNA glycosylase independently of DNMT1 and DNMT3B in cancer cells. *Int J Oncol* 2010;36:1563–1572.
17. Milutinovic S, Brown SE, Zhuang Q, *et al*. DNA methyltransferase 1 knock down induces gene expression by a mechanism independent of DNA methylation and histone deacetylation. *J Biol Chem* 2004;279:27915–27927.
18. Kawamoto K, Hirata H, Kikuno N, *et al*. DNA methylation and histone modifications cause silencing of Wnt antagonist gene in human renal cell carcinoma cell lines. *Int J Cancer* 2008;123:535–542.
19. Esteller M. Cancer epigenomics: DNA methylomes and histone-modification maps. *Nat Rev Genet* 2007;8:286–298.
20. Hirst M, Marra MA. Epigenetics and human disease. *Int J Biochem Cell Biol* 2009;41:136–146.
21. Feng W, Yonezawa M, Ye J, *et al*. PHF8 activates transcription of rRNA genes through H3K4me3 binding and H3K9me1/2 demethylation. *Nat Struct Mol Biol* 2010;17:445–450.
22. Esteller M. Epigenetics in cancer. *N Engl J Med* 2008;358:1148–1159.
23. Jung Y, Park J, Kim TY, *et al*. Potential advantages of DNA methyltransferase 1 (DNMT1)-targeted inhibition for cancer therapy. *J Mol Med* 2007;85:1137–1148.
24. Song SH, Kim A, Ragoczy T, *et al*. Multiple functions of Ldb1 required for beta-globin activation during erythroid differentiation. *Blood* 2010;116:2356–2364.
25. Nam HJ, Kim HP, Yoon YK, *et al*. Antitumor activity of HM781-36B, an irreversible Pan-HER inhibitor, alone or in combination with cytotoxic chemotherapeutic agents in gastric cancer. *Cancer Lett* 2011;302:155–165.
26. Goll MG, Bestor TH. Eukaryotic cytosine methyltransferases. *Annu Rev Biochem* 2005;74:481–514.
27. Chen T, Li E. Establishment and maintenance of DNA methylation patterns in mammals. *Curr Top Microbiol Immunol* 2006;301:179–201.
28. Shah MY, Vasanthakumar A, Barnes NY, *et al*. DNMT3B7, a truncated DNMT3B isoform expressed in human tumors, disrupts embryonic development and accelerates lymphomagenesis. *Cancer Res* 2010;70:5840–5850.
29. Ghoshal K, Motiwala T, Claus R, *et al*. HOXB13, a target of DNMT3B, is methylated at an upstream CpG island, and functions as a tumor suppressor in primary colorectal tumors. *PLoS One* 2010;5:e10338.
30. Girault I, Tozlu S, Lidereau R, *et al*. Expression analysis of DNA methyltransferases 1, 3A, and 3B in sporadic breast carcinomas. *Clin Cancer Res* 2003;9:4415–4422.
31. Noshu K, Shima K, Irahara N, *et al*. DNMT3B expression might contribute to CpG island methylator phenotype in colorectal cancer. *Clin Cancer Res* 2009;15:3663–3671.
32. Feltus FA, Lee EK, Costello JF, *et al*. DNA motifs associated with aberrant CpG island methylation. *Genomics* 2006;87:572–579.
33. Bai S, Ghoshal K, Datta J, *et al*. DNA methyltransferase 3b regulates nerve growth factor-induced differentiation of PC12 cells by recruiting histone deacetylase 2. *Mol Cell Biol* 2005;25:751–766.
34. Cruz JJ, Ocana A, Del Barco E, *et al*. Targeting receptor tyrosine kinases and their signal transduction routes in head and neck cancer. *Ann Oncol* 2007;18:421–430.
35. Annemans L, Van Cutsem E, Humblet Y, *et al*. Cost-effectiveness of cetuximab in combination with irinotecan compared with current care in metastatic colorectal cancer after failure on irinotecan—a Belgian analysis. *Acta Clin Belg* 2007;62:419–425.
36. Xiong HQ, Rosenberg A, LoBuglio A, *et al*. Cetuximab, a monoclonal antibody targeting the epidermal growth factor receptor, in combination with gemcitabine for advanced pancreatic cancer: a multicenter phase II Trial. *J Clin Oncol* 2004;22:2610–2616.
37. Hu K, Li SL, Gan YH, *et al*. Epiregulin promotes migration and invasion of salivary adenoid cystic carcinoma cell line SACC-83 through activation of ERK and Akt. *Oral Oncol* 2009;45:156–163.
38. Zhuang S, Yan Y, Daubert RA, *et al*. Epiregulin promotes proliferation and migration of renal proximal tubular cells. *Am J Physiol Renal Physiol* 2007;293:F219–F226.
39. Feinberg AP, Tycko B. The history of cancer epigenetics. *Nat Rev Cancer* 2004;4:143–153.
40. Jaenisch R, Bird A. Epigenetic regulation of gene expression: how the genome integrates intrinsic and environmental signals. *Nat Genet* 2003;33(Suppl):245–254.
41. Kotake Y, Zeng Y, Xiong Y. DDB1-CUL4 and MLL1 mediate oncogene-induced p16INK4a activation. *Cancer Res* 2009;69:1809–1814.
42. Harrington KJ. Rash conclusions from a phase 3 study of cetuximab? *Lancet Oncol* 2010;11:2–3.
43. Robak T. New nucleoside analogs for patients with hematological malignancies. *Expert Opin Investig Drugs* 2011;20:343–359.